Validation of ELP Dosimetry Using PRESAGE Dosimeter

by

Kara Michelle Lambson

Medical Physics Graduate Program
Duke University

Date:_____

Approved:

_____
Jing Cai, Supervisor

_____
Mark Oldham

_____
Robert Reiman

Thesis submitted in partial fulfillment of
the requirements for the degree of Master of Science
in the Graduate Program in Medical Physics in
the Graduate School of Duke University

2017

ABSTRACT

Validation of ELP Dosimetry Using PRESAGE Dosimeter

by

Kara Michelle Lambson

Medical Physics Graduate Program
Duke University

Date:_____

Approved:

_____
Jing Cai, Supervisor

_____
Mark Oldham

_____
Robert Reiman

Thesis submitted in partial fulfillment of
the requirements for the degree of Master of Science
in the Graduate Program in Medical Physics in
the Graduate School of Duke University

2017

Abstract

The purpose of this research is to validate the use of a PRESAGE dosimeter as a method to quantitatively measure dose distributions of injectable brachytherapy based on elastin-like polypeptide (ELP) nanoparticles. ELP has several useful properties for treatment purposes, including the ability to be tagged with a radioactive element, an inverse temperature phase transition useful for self-assembly into hydrophobic aggregation upon injection, and a highly tunable threshold temperature based on the amino acid composition and concentration. PRESAGE is a solid, transparent polyurethane-based dosimeter whose dose is proportional to a change in optical density, making it useful for visualizing the dose from a radionuclide-tagged-ELP injection. Initial experiments with the gel phantoms demonstrate viability for assessing I-125 dose deposition, as the image analysis showed the similar relative dose distributions compared with a MATLAB simulation.

Contents

List of Figures

Acknowledgements

I would like to thank my advisor, Dr. Jing Cai, for his help and guidance during the entirety of this thesis project. Additionally, I would also like to thank for following people, without whom my project would not have happened:

- Kyle Lafata for his mentorship and willingness to share his extensive knowledge on this subject.
- Jeff Schaal, Devin Miles, and Paul Yoon for providing input and being very helpful collaborative partners in this novel experimental work.
- My committee members, Dr. Mark Oldham and Dr. Robert Reiman, for their advice and assistance during the write-up process.

1. Introduction

1.1 Motivation

Injectable brachytherapy using elastin-like polypeptides (ELP) is a promising new technique that may one day be a useful new method for radiation treatment of cancer. One of the primary focuses of research involving drug delivery for cancer therapy is aiming to improve the therapeutic index by increasing the amount of treatment delivered to the tumor site and decreasing the exposure to healthy tissues.[1] A unique feature of ELPs is their inverse temperature phase transition, i.e. they are in liquid form below the threshold temperature and insoluble above. This serves as a useful property for treatment purposes, as the genetically encoded polymer solution composed of radiolabeled-ELP will self-assemble into a hydrophobic aggregation upon injection into a tumor.

Some suggested applications for these polypeptide injections include treating early-stage patients without requiring radical surgery, making unresectable tumors such as those near to major arteries or organs operable by shrinking them down to more manageable sizes, or to improve the quality of life for patients with advanced tumors.[2] Currently however, unlike brachytherapy seeds, the true distribution of dose is difficult to predict which prevents definitive pre-planning. Dosimetry techniques, namely the use of PRESAGE, are currently being explored in order to obtain an accurate dose distribution of the radioactivity. Developing the ability to pre-plan ELP brachytherapy

procedures based on a series of injection parameters would be essential to progressing this novel therapy technique.[20]

1.2 Objectives

The primary aim of this study is to investigate the feasibility of a PRESAGE phantom in measuring dose distributions of injectable brachytherapy based on ELP nanoparticles. Previous studies have confirmed the effectiveness of radiolabeled-ELP solution as a means to deposit internal radiation to a tumor, but methods to determine the dose distribution upon injection are lacking. Therefore, an experimental design using PRESAGE, a 3D radiochromic dosimeter, and radionuclide-tagged ELP has been created and implemented. Since PRESAGE as a means to determine dose from low-energy brachytherapy sources has not been thoroughly studied, a MATLAB simulation using a point-dose kernel modeling the experiment was incorporated into the workflow to validate the experiment.

1.3 PRESAGE Dosimeter

The PRESAGE® 3D dosimeter is composed of polyurethane, radiochromic components, and halogen-containing free radical initiators such as leucodye that cause a change in optical absorbance after exposure to ionizing radiation.[3] By quantifying this change in optical density, the radiation dose may be determined via a calibration factor obtained by determining the change in optical density as a function of ionizing radiation dose. Typically, PRESAGE has a linear response over a wide range of doses, making it a

useful tool for visualizing dose, as the density of green will be directly proportional to the exposure due to the radiolytic oxidation of the leucodye.[4] The dose response sensitivity can be adjusted by changing the proportions of the leucodye and the initiating agent components.[5] The composition also influences the water equivalency, though when used for clinical radiation dosimetry purposes, the dosimeter should ideally exhibit radiological properties that are tissue equivalent over the energy range of the radiation being used. This equivalency allows the dosimeter to be used as a phantom.

One concern however is the water equivalency and energy sensitivity at very low photon energies and whether or not some versions of the deformable PRESAGE formulations would be adequately stable for prolonged irradiation. Adamson et al effectively showed that current deformable formulations have nearly water equivalent attenuation properties for I-125, the radionuclide being used in this study, though further investigation of the stability over time is needed. A lack of water equivalency may be corrected with the relevant dosimetric correction factor to convert the dose measured by the dosimeter to the absorbed dose in water.[4] Overall, despite not being widely used, 3D dosimetry using polyurethane based dosimeters with optical CT shows promising results as a means to verify dosimetric distributions surrounding low energy brachytherapy sources due to its ability to verify high-spatial resolution dose distributions calculated using Monte Carlo simulations.[7]

Additional advantages of PRESAGE include its machinability and the insensitivity to oxygen contamination, meaning an external container or phantom material is not required in the lab environment. During the molding process, a wide variety of shapes and sizes are achievable, making it a viable option for many applications.[4] Also, the radiochromic color change absorbs light rather than scatters it, which facilitates high accuracy readout by optical CT.[5] While there is no atmosphere sensitivity, the samples and phantoms should be kept in dark conditions during investigation to protect from visible and ultraviolet light that may induce color change. The gold standard to obtain the radiation induced change in optical density is a volume-averaged readout by a spectrophotometer using the peak absorption wavelength of 633nm, as seen in Fig.1. This method can be used for the calibration of the phantom by using cuvette samples from the same batch. For analysis of color change in the phantom, a line profile readout of the optical density by 2D projection imaging can be determined by utilizing a high-resolution telecentric optical system.[8]

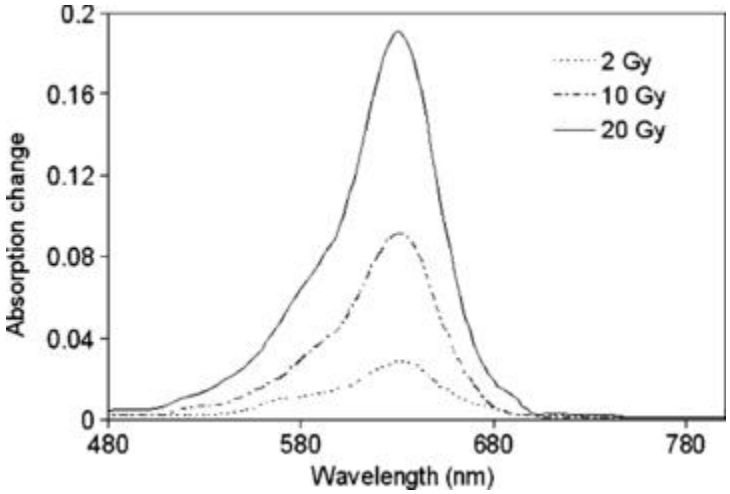

Figure 1: Spectra of absorption changes for different radiation doses.[4]

1.4 Elastin-like Polypeptides

There are many unique features that make elastin-like polypeptides (ELP) an attractive method for a variety of different treatments. ELPs are composed of Val-Pro-Gly-Xaa-Gly (VPGXG) pentapeptide chains that give the characteristic inverse transition temperature, where the ELPs are soluble in aqueous solution below the inverse transition temperature and form an insoluble, polymer-rich aggregation above.[9] This is determined by the Xaa component, a guest residue that can be any naturally occurring amino acid except proline.[10] This transition is reversible, and the ELP will re-dissolve when the solution temperature is lowered below the threshold. The threshold temperature T_t is determined by the amino acid sequence composition and the chain length of the ELP and is tunable, making their applications versatile and easily optimized for specific drugs or patient-specific thermal and environmental cues. The ELP can be designed to exhibit a T_t between 37°C and 42°C and can be designed to be

soluble and injectable at room temperature but solidify at physiological body temperatures.[1] A hydrophobic group in the guest residue position will lower the phase transition temperature, while a hydrophilic group will increase it. The phase transition properties of ELP remain even when fused to another protein or molecule, a feature that makes it a molecule of interest for many drug delivery applications.[11]

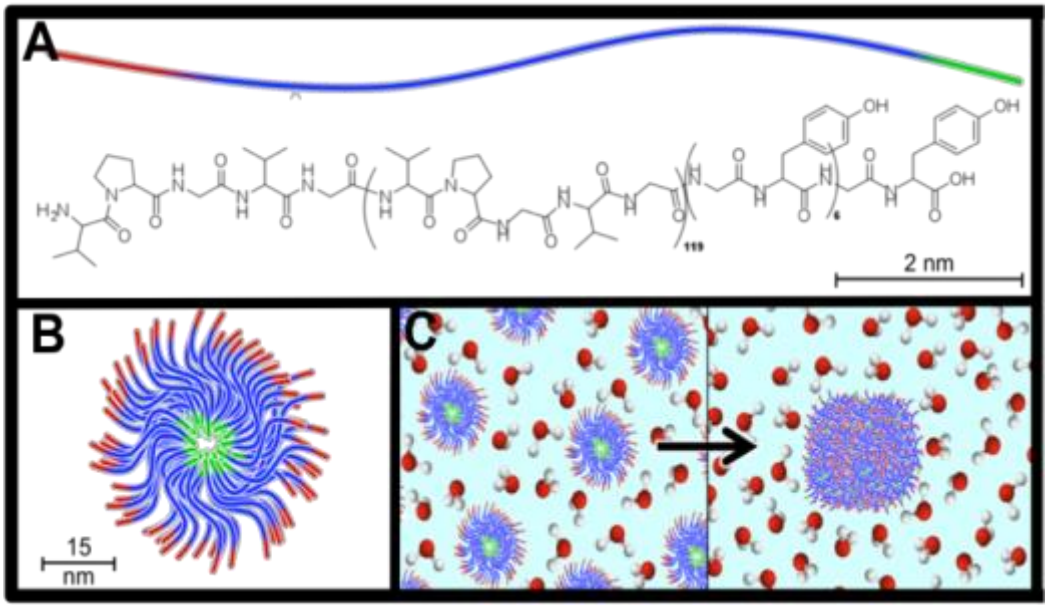

Figure 2: A,B) Generic ELP nanoparticle design. The green segment represents hydrophobic region within the polymer, red represents hydrophilic. C) Demonstration of inverse temperature phase transition. Left shows ELP in soluble form in temperatures below threshold, right shows single hydrophobic aggregation when warmer than transition temperature.[20]

In addition to the biocompatibility feature of ELPs, another benefit is the biodegradation over time that makes it useful for *in vivo* application such as brachytherapy. Brachytherapy is a clinical technique used for a variety of cancers such as prostate or cervical where a tumor is selectively exposed to large doses of radiation via locally implanted "seeds".[2] Whereas traditional brachytherapy seed placement may

result in permanent seed placement or occasional need for post-treatment excision, radionuclide-tagged ELP may overcome these limitations with non-toxic products that will reabsorb into the body after the radioactivity has decayed to safe levels that no longer pose a threat of systemic toxicity. Depending on the composition of the ELP, the injections can have a lifespan *in vivo* that is compatible with the radionuclide used for treatment.

While the brachytherapy technique remains popular and effective for a variety of treatments like prostate cancer, there is a small risk of seed migration away from the intended target volume location. This may result in adverse radiation exposure to unintended targets in addition to not depositing the full dose coverage to the target, which translates to inadequate dosimetry and risk of eventual treatment failure.[12] This risk would be minimized when using ELP, as the radioactive volume will immediately aggregate upon injection and stay localized within the tumor with minimal systemic toxicity. Additionally, the injection would be applied via a high gauged needle, taking away the need for the larger diameter catheters used for seed placement.

1.5 Point-Dose Kernel for Internal Dosimetry

In order to validate the experimental model, a simulation of the phantom using a point-dose kernel to get a 3D absorbed dose distribution was performed to compare the relative dosimetry. Point-dose kernel convolution techniques have been extensively researched and validated so as to give a more accurate dose calculation that does not

rely on the assumptions of a standard geometry and uniform activity distribution.[18] The radionuclide kernel K(r) is defined as the absorbed dose per decay at a point r away from the source. The absorbed dose within a volume can be calculated typically for a point of activity at the center of the sphere and is defined for the different radionuclides.[19] The algorithm has been validated through a series of Monte Carlo simulations and are used to generate 3D dose maps.

The dose calculation algorithm has been developed based on the point-dose kernel convolution techniques, which take an activity map and convert it to dose via a series of calculations in frequency space using Fourier transforms. In internal radiation dosimetry calculations that use this formalism, the linear response function is assumed to be a point-dose kernel that describe a system's impulse response to the decay of a specific radionuclide, or the isotropic dose distribution from a point source of radiation within a uniform medium.[20] Using the point-dose convolution method specified for I-125, the expected dosimetry from an ELP injection within a medium can be pre-calculated. The advantages to this method are that it is computationally efficient and gives the ability to calculate dose from non-homogenous activity concentrations. It has been previously used in Liu et al's I-125-tagged ELP animal study, where the input activity map was a heterogeneous distribution shown in Figure 3 acquired via a microspect scanner. However, it is limited in that it only considers homogenous media and has problems at tissue interfaces. Running a Monte Carlo simulation for

heterogeneous media would avoid those problems but it would no longer be computationally efficient. For the purposes of this thesis work, the assumption of homogenous media is reasonable, as PRESAGE has water equivalent properties.

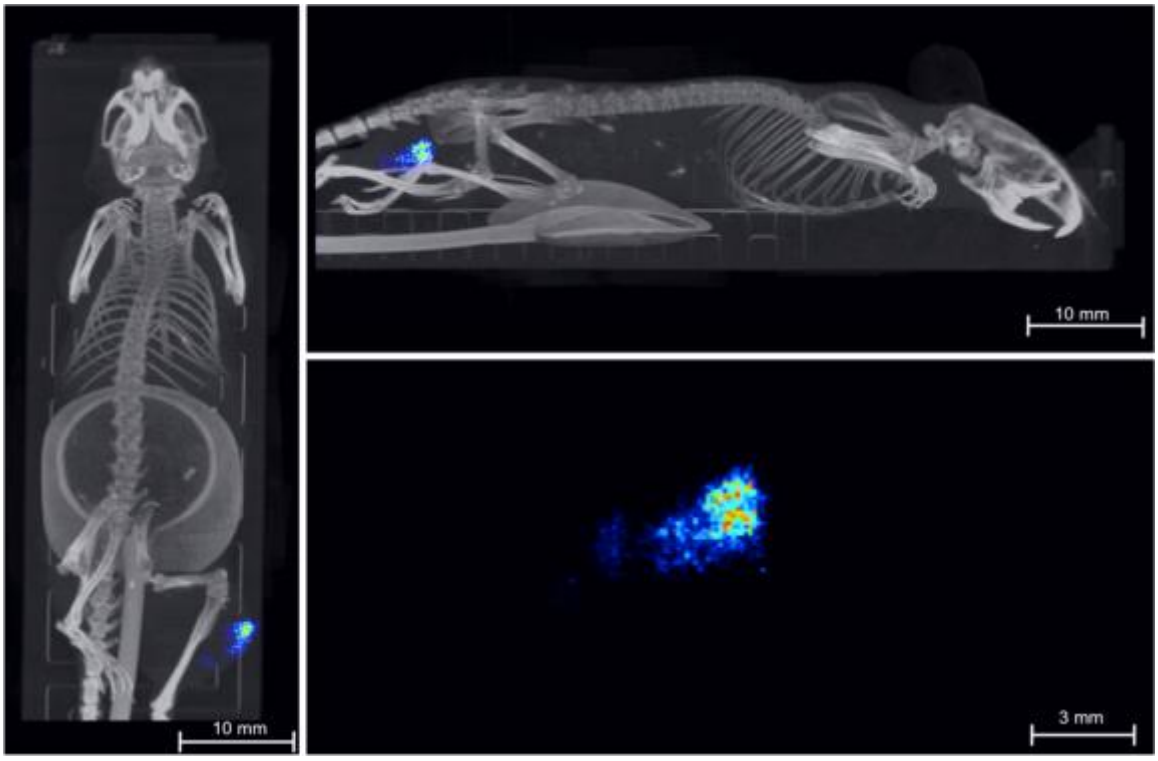

Figure 3: Activity map of I-125 tagged ELP injection in mouse tumor. [20]

2. Methods

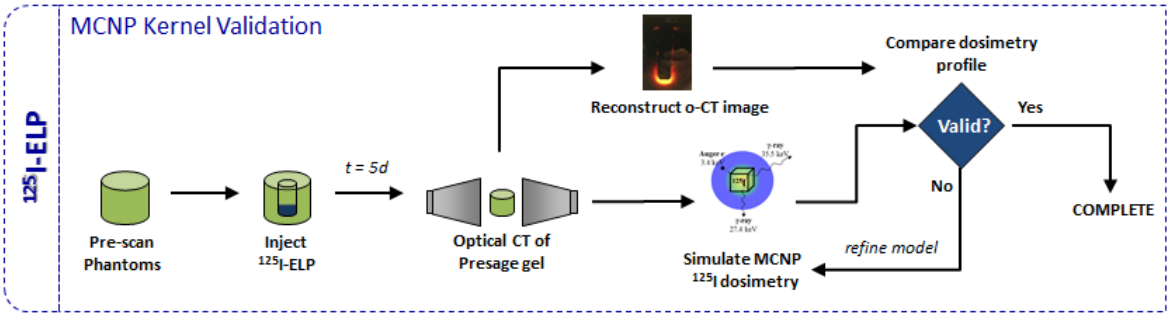

Figure 4: Overview of experimental and simulation process. The implementation is discussed in detail in the Methods section. (*Permission acquired from Jeff Schaal)*

2.1 PRESAGE Phantom Design and MATLAB Simulation

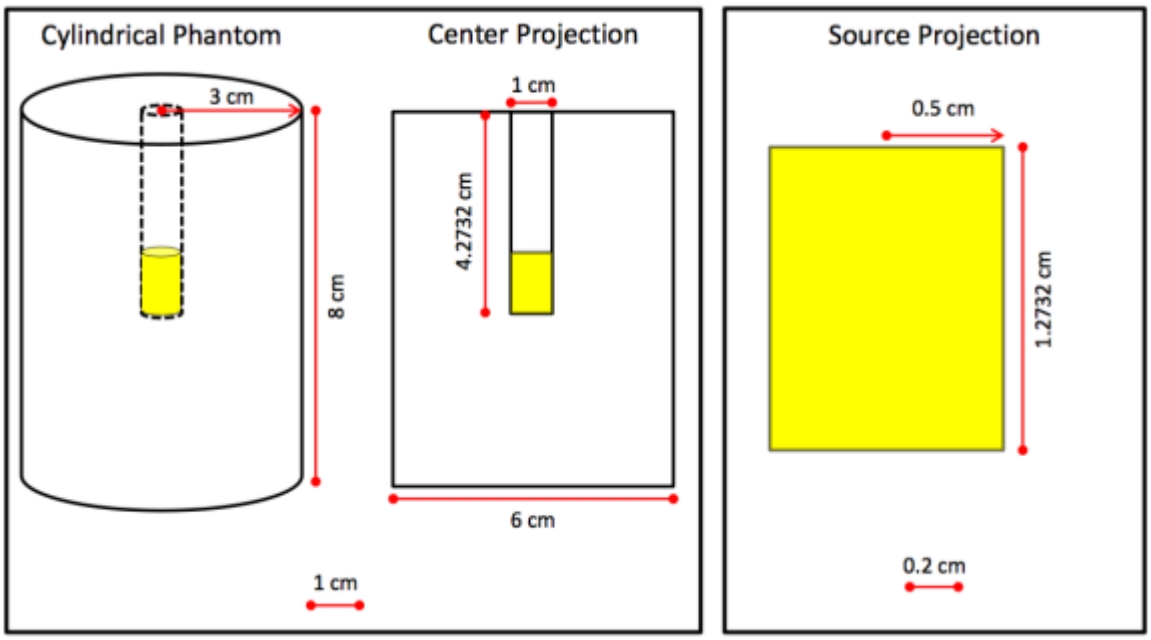

Figure 5: Schematic of PRESAGE phantom with 1cc ELP volume

A cylindrical phantom made of the radiochromic PRESAGE material was designed in order to allow for the simplest geometry to verify the agreement between

the experiment and MATLAB simulation. A 1cm diameter and 4.27cm deep cavity was set into the center during the PRESAGE molding process to enable the insertion of the source geometry with a 1cc injection volume. The 1cc injection is composed of both the saline solution and the radionuclide-tagged ELP, with the amount of ELP in the solution determined by the desired activity, in this case 1mCi.

One factor that had to be taken into account was the effect of gravity on the aggregation of ELP in the saline solution during the 5-day irradiation period since the phantom would be kept in an upright immobile position over the course of the exposure. This would influence the MATLAB simulation phantom, as the source would be smaller and the radioactivity more concentrated, thereby assigning more activity to each of the source voxels. A supplemental experiment using a known concentration of un-tagged ELP was performed to see how quickly the ELP would solidify in the saline solution. The set-up and observations for this experiment are shown in Figure 5. Based on the results, the simulation size of the source was adjusted accordingly and the activity increased per voxel to give a total activity of 1mCi for the whole 1cc source. The activity per voxel was calculated by first determining how many voxels were in the volume, assuming that each voxel is $1mm^3$. The diameter of the cavity was 10 voxels and the height of the source was changed to 6 voxels. Therefore, the total volume of voxels is $\pi r^2 h$ in mm^3, or 1.5π mm^3 and the activity per voxel is $0.001mCi/mm^3/4.71mm^3$, or 0.000212mCi/voxel.

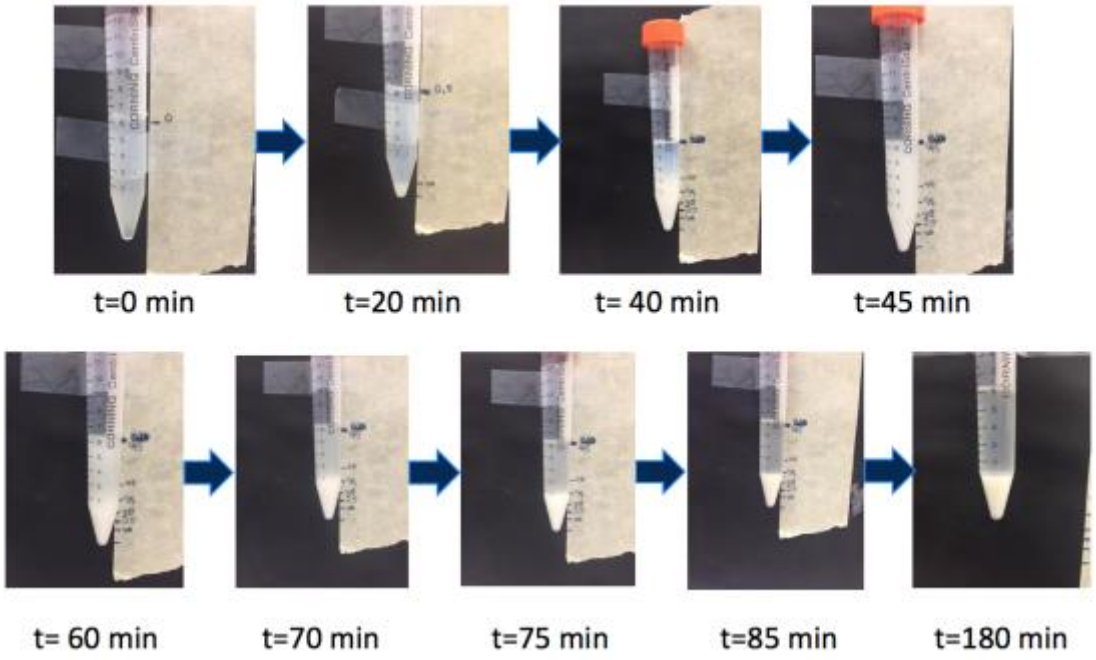

Figure 6: Gravity effect on aggregation of ELP suspended in saline solution

The determination of the activity of the solution used TG-43 formulism to solve for the necessary amount of time required to get 1 Gy of dose 1 cm away in the phantom. This calculation takes into account numerous parameters specific to certain radionuclides, in this case Iodine-125. With point source geometry, the dose rate approximation at a distance away is calculated with the following formula:

$$\dot{D}(r) = S_K * \Lambda * \left(\frac{r_0}{r}\right)^2 * g_p(r) * \overline{\phi_{an}} \qquad \text{[Eq 2.11]}$$

where S_K is the air-kerma strength in μGy m^2/hr, Λ is the dose rate constant of the radionuclide in cGy/hr/U (where U is the known air kerma strength), $1/r^2$ is the inverse square correction where r is the distance from the source center in cm, r_0 is the reference distance of 1cm, $g_P(r)$ is the radial dose function describing the dose rate at a distance r

from the source relative to the dose rate at r_0 assuming the source can be represented as a point, and $\overline{\phi_{an}}$ is the anisotropy constant. These values are tabulated in the TG-43 report and may be used to obtain the dose rate at any distance r from the source.

This dose rate can be used to calculate the expected dose after a 5-day incubation period:

$$Dose = \dot{D}(r) * 1.44 * t_{\frac{1}{2}} * (1 - e^{\frac{-\ln(2)t}{t_{\frac{1}{2}}}}) \quad \text{[Eq 2.12]}$$

where $t_{1/2}$ is 59.9 days (the half-life of I-125), and t is the 5-day total time of exposure. After converting to dose for each voxel in the 3D phantom, the dose in the cavity can be set to 0 since there is no longer any radioactivity remaining.

For 2D analysis, the difference of the normalized output dose maps of the reconstruction and simulation images may be computed and imaged to observe the discrepancy between the two. Then, a line profile can be drawn across any slice to observe the dose fall off as the distance from the source increases. For consistency between the simulation and the reconstruction, a slice just below the cavity is selected, a value that is determined by the number of pixels and resolution. These values are one 1mm pixel away for the simulation and ten pixels (each 0.1mm) away in the reconstructed image. For relative dosimetry comparison with the reconstructed CT data, the data can be normalized by dividing each pixel by the maximum pixel value along the slice of interest.

2.2 Calibration

The calibration procedure for calculating absolute dose from optical density was adapted from Jackson et al, where small volumes of PRESAGE in optically clear cuvettes from the same batch as the phantom are placed in solid water at a known depth and surrounded by bolus material to ensure good scatter conditions. The setup is shown in Figure 7 below. The cuvettes are scanned before and after irradiation using a spectrophotometer to obtain the change in absorbency, which corresponds to the optical density. Each cuvette was exposed to varying levels of radiation from 0 to 35.9 Gy using a linear accelerator, with two cuvettes at each dose. A linear calibration curve was then obtained by plotting optical density versus the known dose, from which the sensitivity can be obtained by finding the slope. The average optical density value was taken between the cuvettes of the same exposure.

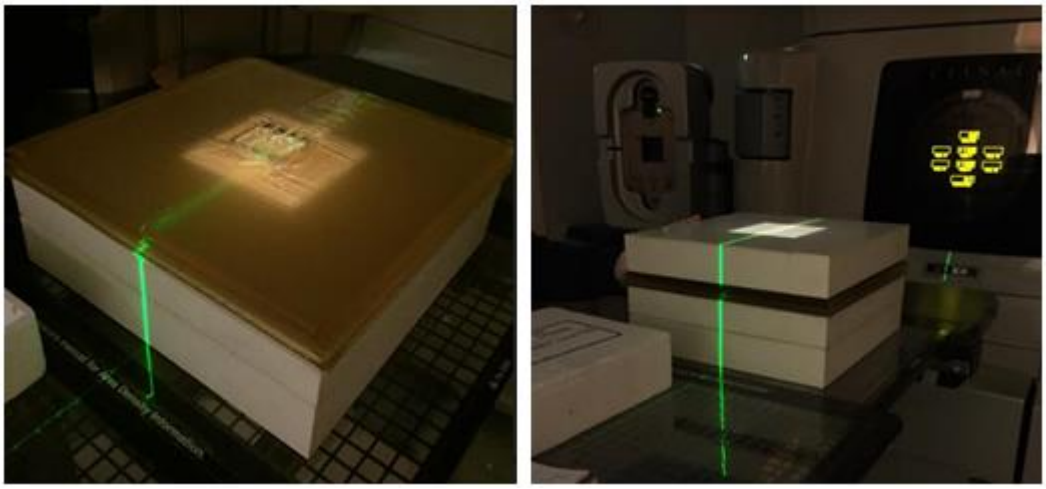

Figure 7: Setup for calibration of cuvettes with bolus and solid water.

2.3 Optical CT Imaging System

A pre-optical CT scan was performed to get the baseline tomographic optical density before irradiation. The scan was performed with the 2D projection telecentric optical system developed at Duke, the Duke Micro Optical Scanner (DMicrOS), the system of which is shown in Figure 8. This system uses a 2W LED light source behind a narrow band filter, giving the source a uniform flood field with a wavelength of 633nm, the peak absorbency for the PRESAGE. The telecentric lens ensures a collimated light field where the dosimeter can be imaged without object magnification effects, and the imaging lens minimizes scattered light contributions.

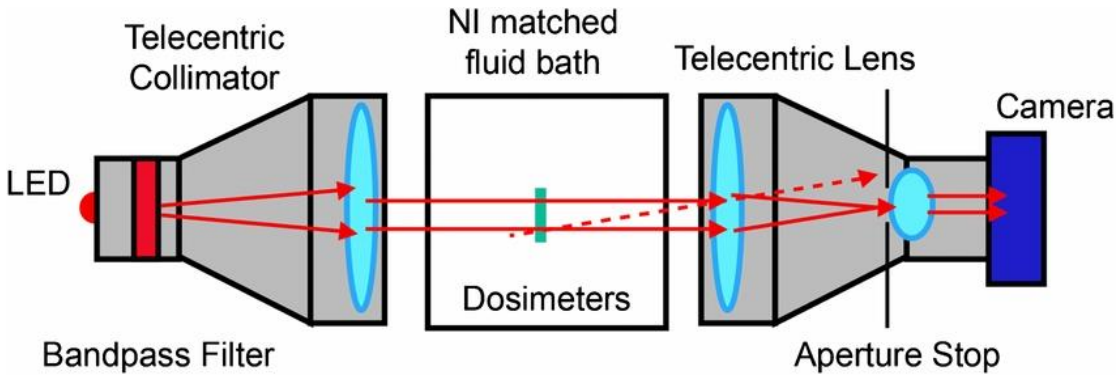

Figure 8: Diagram of the Duke Micro Optical Scanner (DMicrOS) System used to determine the change in optical density [8]

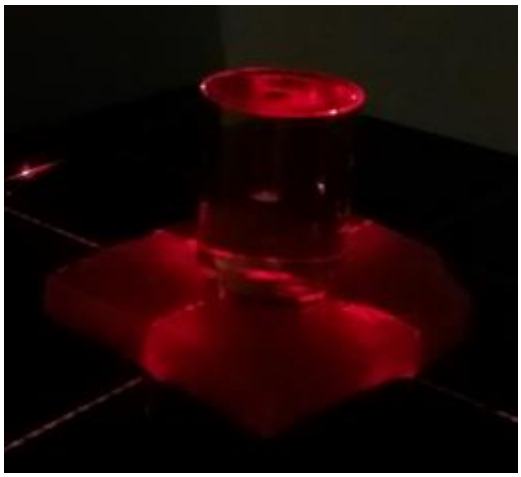

Figure 9: Pre-optical CT scan of phantom to obtain baseline tomographic optical density

For the optical CT pre-irradiation scan of the dosimeter, the procedure detailed in Adamson was used. The scan was acquired using the DMicrOS scanning system with the channel immersed in a refractive fluid containing a mixture of mineral oil, as shown in Figure 8. The fluid was then removed before insertion of the source into the channel. After exposure, the post-irradiation optical CT scan was acquired in the same way with the same refractive fluid and the dosimeter immersed. The resultant images allowed for 3D dose distribution reconstruction after image registration.

2.4 Injection and Image Reconstruction

After pre-scans and calibration were completed, 1cc of I-125 tagged ELP solution was injected into the cavity and left in place for 5 days. The tagged ELP was then removed from the cavity using 1M NaOH and scanned again to obtain the post-optical-CT image. A graphical user interface was created in MATLAB to obtain an accurate

registration between the pre- and post-scan images.[8] The differential optical density dataset was generated by subtracting the pre-irradiation OD image from the post-irradiation image. This dataset and the corresponding images were then uploaded to MATLAB to convert OD to dose and obtain line profiles across selected regions of interest. To validate the process, these line profiles were compared with line profiles from the point-dose kernel convolution simulation.

2.4 Dose Calculation Algorithm for Simulation

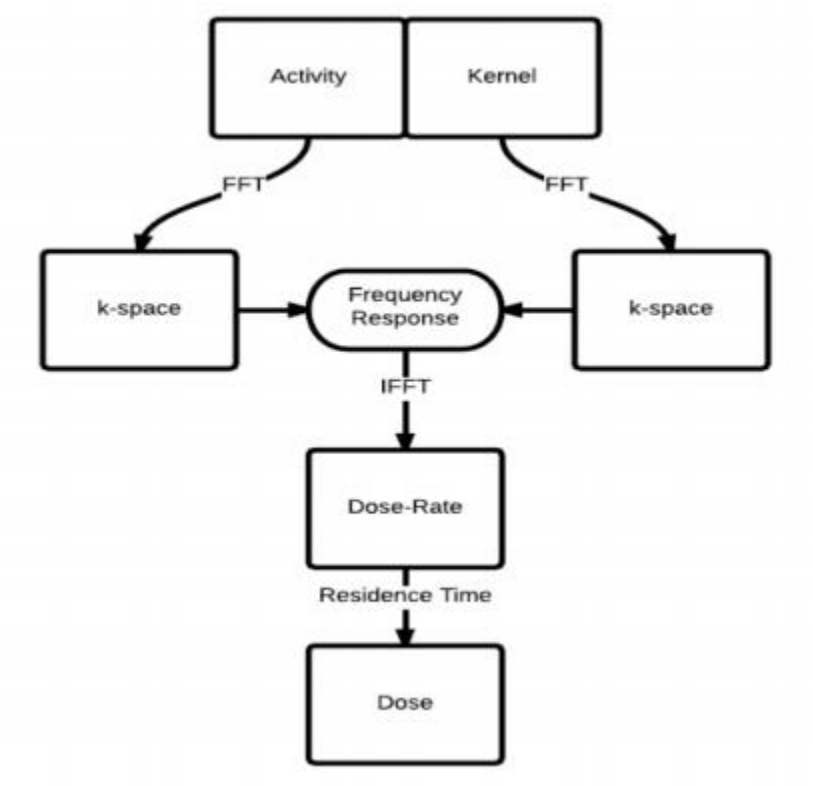

Figure 10: Workflow for dose calculation algorithm. (*Permission acquired from Kyle Lafata)*

For a given radioactivity distribution, the convolution integral is calculated in the frequency domain using fast Fourier transforms. The series of steps is shown in the flow chart in Figure 9. The radionuclide kernel K(r) is defined as absorbed dose per decay at a point r away from the source. In order to get this 3D kernel, a radial dose function like the one shown in Fig. 10 is generated for a point source of I-125 dose distribution in water is used to discretize a distance matrix of the same dimensions as the phantom. Frequency space is re-sampled by padding it with zeros in order to mimimize wrap-around effects in the high frequency regions. A 3D matrix of 199x199x199 elements was pre-allocated for speed with each element representing $1mm^3$ voxel. The center element (100,100,100) was defined as the location of the point-source voxel. Prior to the inverse fast Fourier transform (IFFT) to convert to dose rate, a region of interest in the frequency response of the system is selected to match the 3D field of view of the original activity distribution.[20]

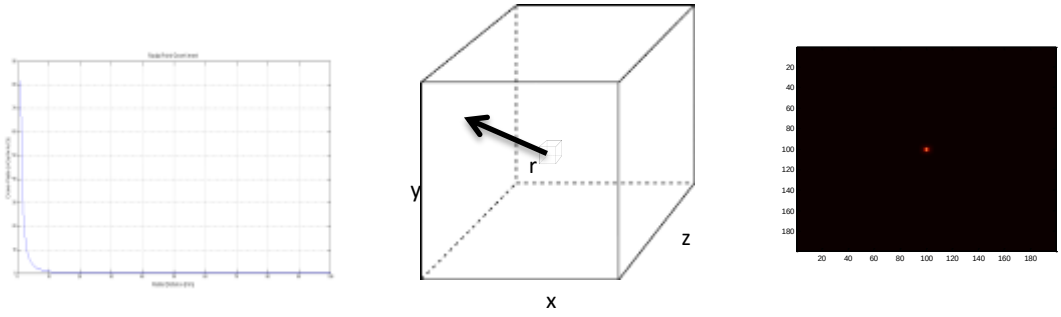

Figure 11: Point-Dose Kernel. A) Radial dose function; B) 3D distance matrix to be filled in with dose as a function of distance values; C) Slice down center of kernel

3. Results

3.1 Calibration

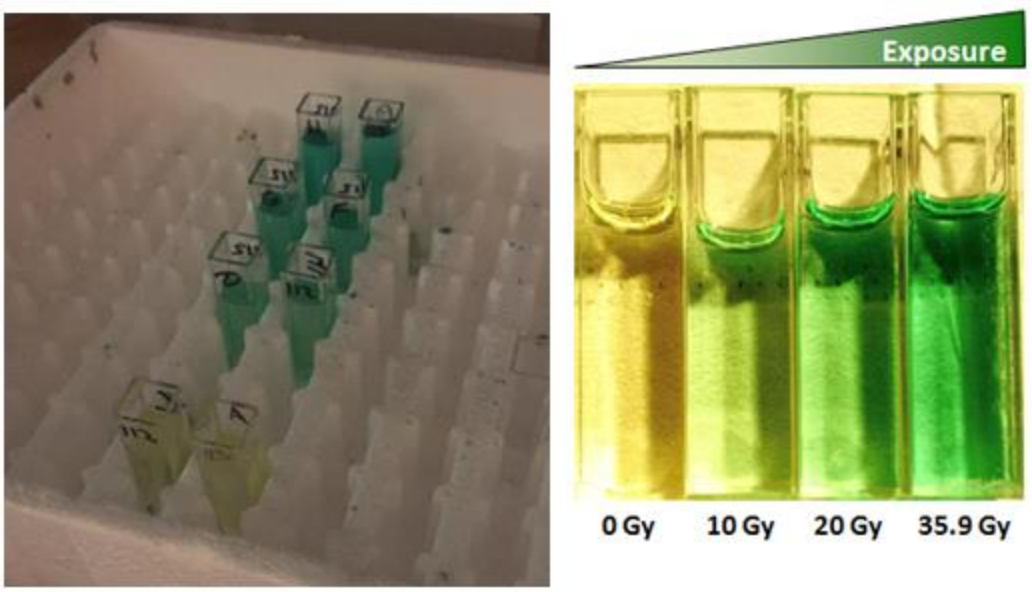

Figure 12: PRESAGE sample cuvettes for calibration

After irradiating the sample cuvettes, each was placed in the spectrophotometer to obtain the absorbency of 633nm light. A plot was generated and the slope obtained to get the calibration factor in change in OD per cm per unit dose. We found this to be 638.2, a value that the image is then multiplied by to get an approximate dose estimate within 5%.[21]

3.2 Experiment

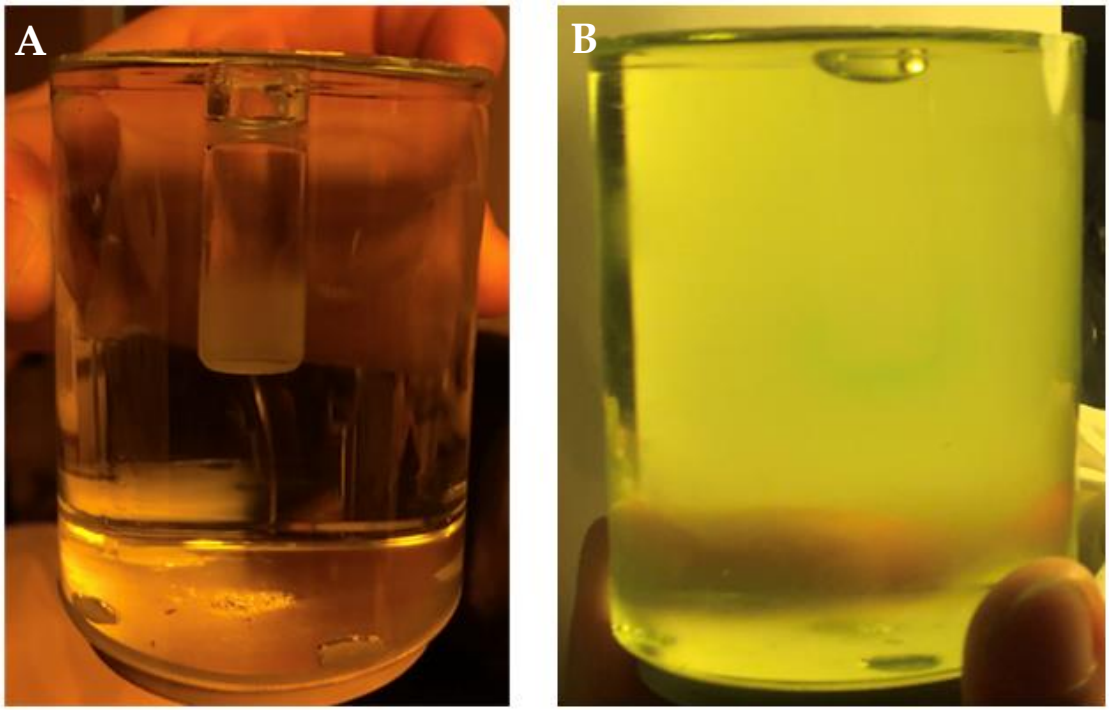

Figure 13: A) 5 days post-irradiation versus B) 12 days post-irradiation. During the week in between observations, the phantom was kept in opaque black bag inside a refrigerator to minimize any color change due to environmental light.

After initial cleansing of the injection cavity, the phantom revealed an opaque white film that obscured the optical CT scan, as seen in Figure 13A. However, upon inspection several days later, the white film was no longer apparent and the optical density change was visible. The phantom with the visible dose provided the optical density change datasets used to obtain line profiles and for further analysis.

3.3 Reconstruction and Simulation

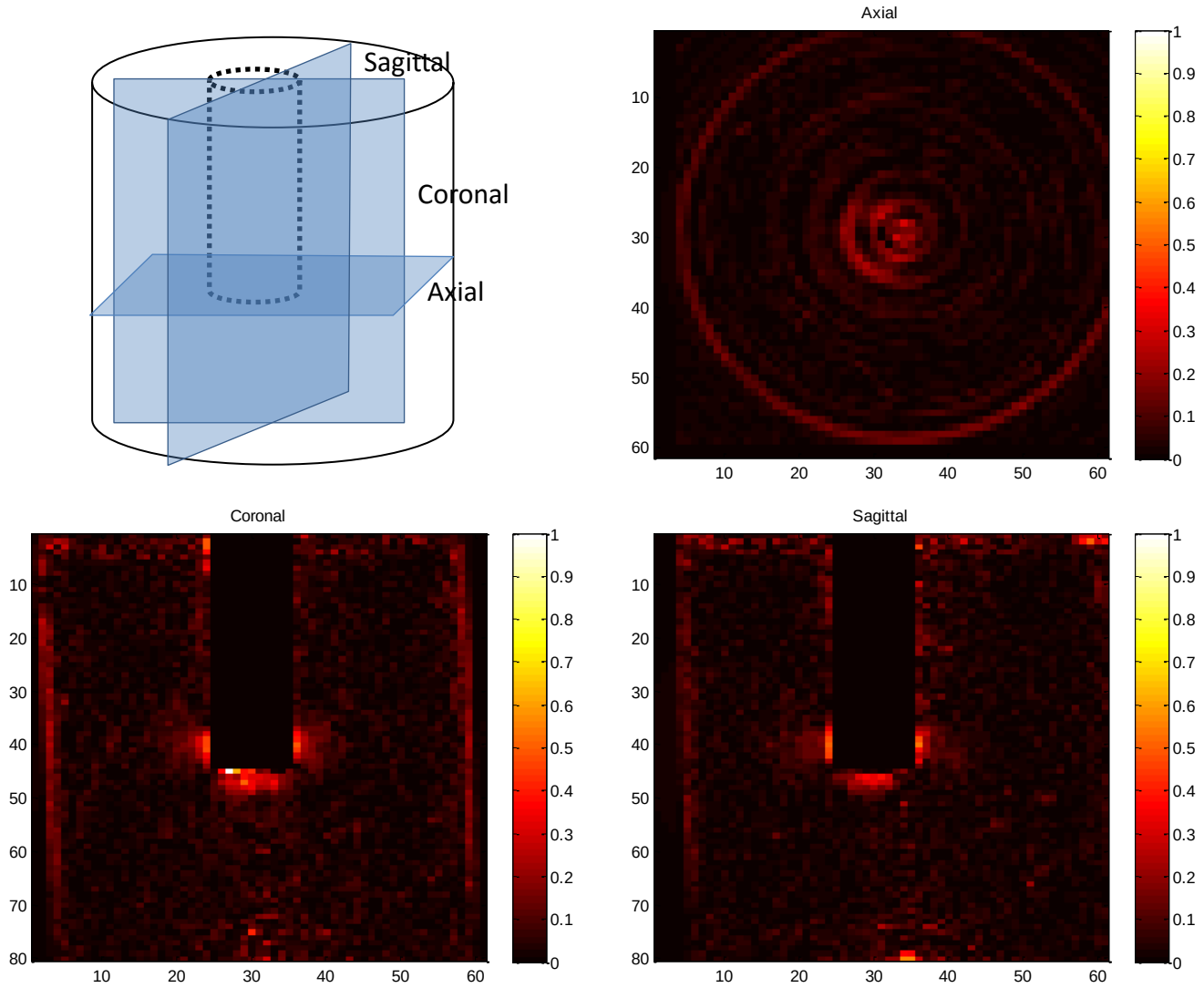

Figure 14: Normalized 2D dose maps illustrating percent difference between simulation and reconstruction in 3 views- sagittal, coronal, and axial. Axial slice acquired 1mm below cavity, coronal and sagittal slices acquired from plane half-way through cavity.

Since the experimental images were of a much higher resolution than the simulation, the matrix was resized to match the dimensions by averaging several pixels. This results in some information loss, but retains enough quantitative data for comparison purposes. Shifts and rotations were performed to overlay the cavities in the reconstruction with the simulation and the values within the cavity were set to 0. If the reconstruction agreed with the simulation perfectly, the intensities of the output pixels in the dose difference map would all be 0. However, since the percent difference is visible, there is a discrepancy between the simulation and reconstruction.

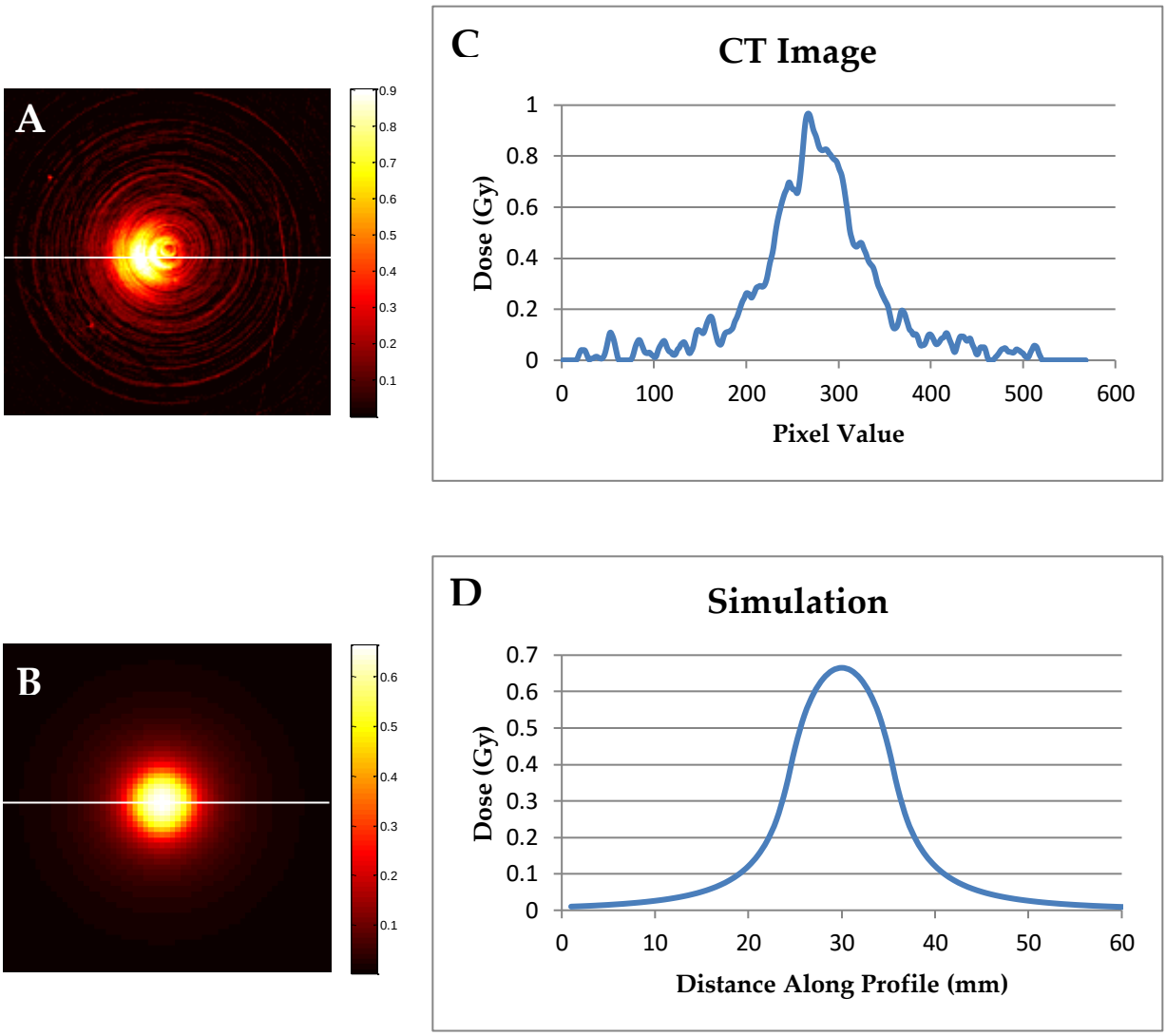

Figure 15: A) The differential optical density image obtained from the image registration of the pre- and post-optical CT scan. The line profile shown in (B) was generated from a line drawn across the center of the dose distribution at a slice 1cm away from the injection site. Image (C) shows the dose distribution as a result of the convolution of the point source with the kernel, the line profile for which is shown in (D)

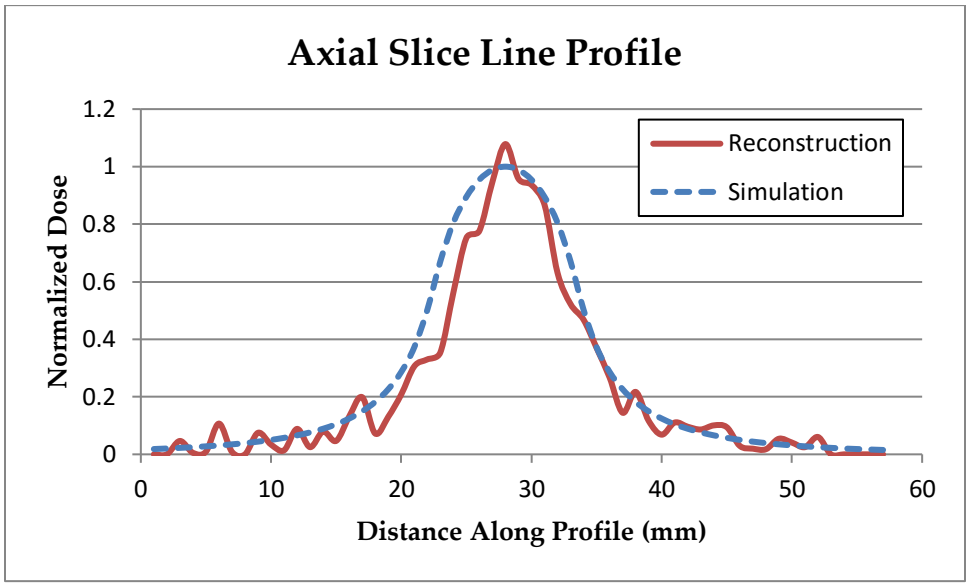

Figure 16: Normalized reconstruction and simulation data at an axial slice directly beneath cavity.

As shown in Figure 15A, the dose distribution in the axial slice beneath the cavity is slightly off-center due to a tilt in the cavity during the molding procedure. The concentric rings around the dose distribution are a result of an imaging artifact from the optical-CT scan. To reduce noise, the line profile was smoothed by taking the average of 10 voxels. The simulation profile was shifted over by 4mm to account for the misalignment of the reconstruction.

In order to compare the relative dose distributions via the normalized data, 1 in every 10 points from the 1x568 reconstruction data was selected in order to obtain the overall profile in comparison with the 1x60 simulation. This results in some data loss, but the overall shape remains the same. The noisier image in Figure 15B shows a more comprehensive dataset for analysis of the dose deposition.

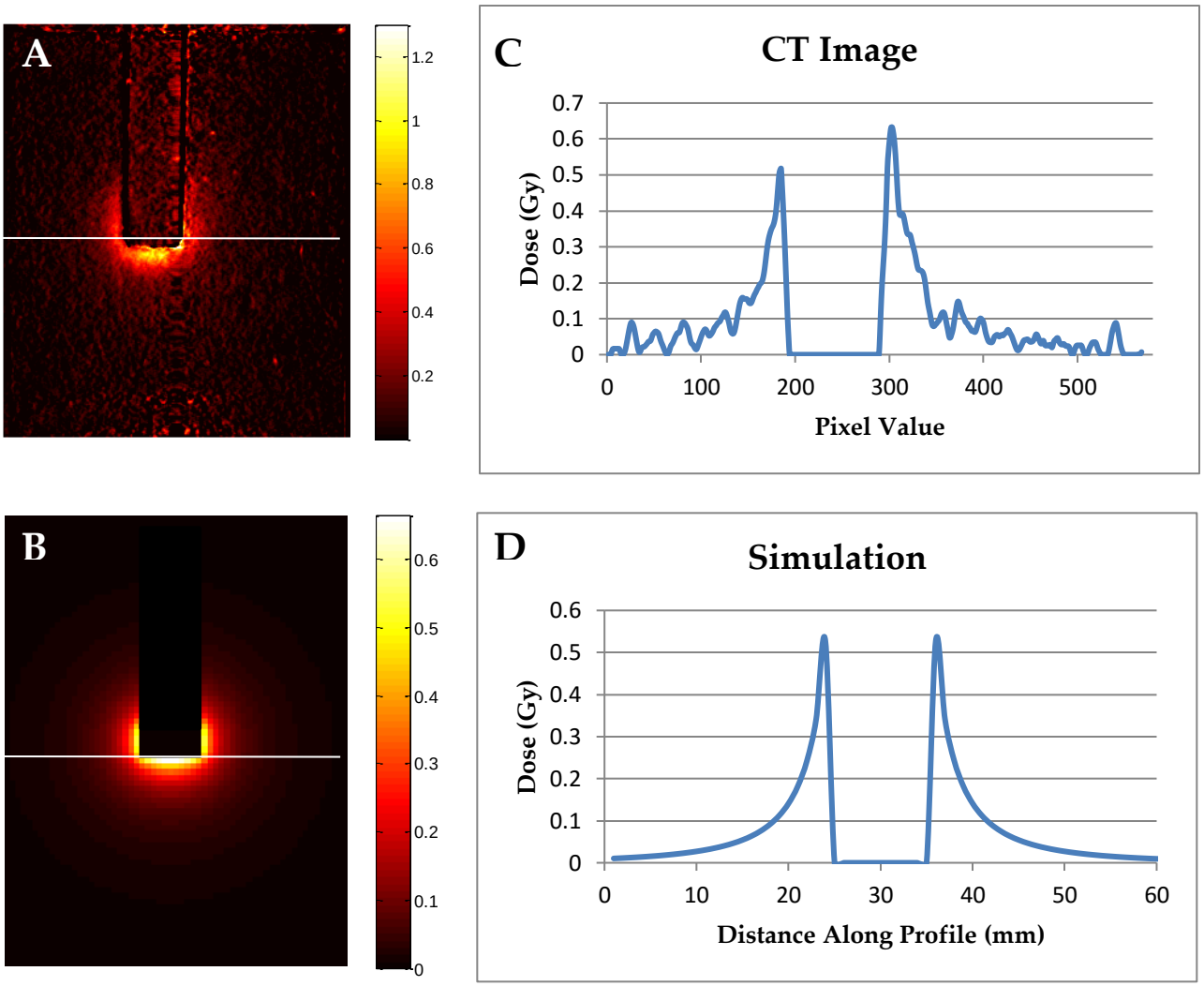

Figure 17: A) The differential optical density image obtained from the image registration of the pre- and post-optical CT scan. The line profile shown in (B) was generated from a line drawn across the dose distribution at a slice close to the base of the cavity. Image (C) shows the dose distribution as a result of the convolution of the point source with the kernel, the line profile for which is shown in (D)

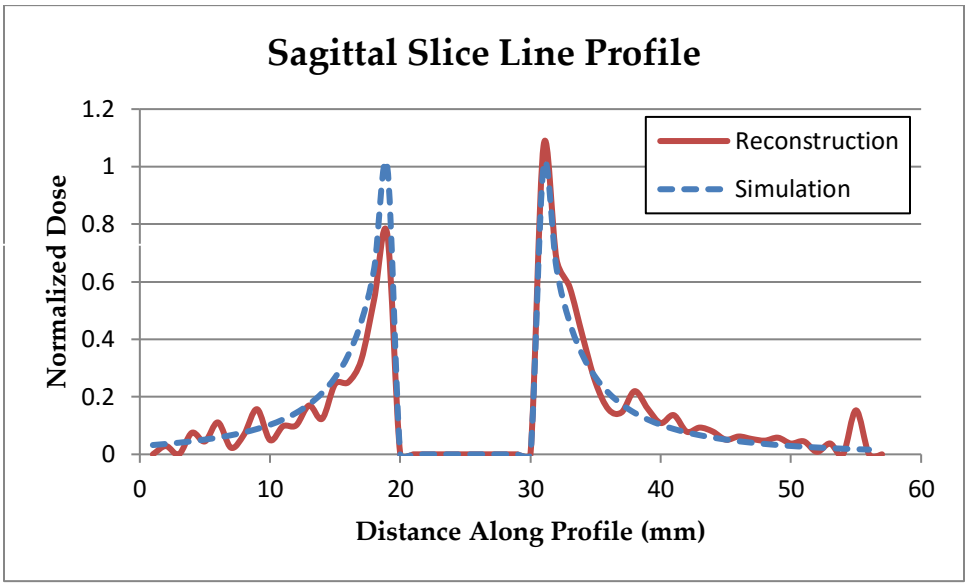

Figure 18: Normalized reconstruction and simulation data at a slice through the sagittal view near the bottom of the injection cavity.

The data for Figure 17B was obtained by taking a line profile across a slice near the base of the injection site. The same noise reduction method as was used for the axial slice profile was applied to smooth the profile and the pixel values within the cavity were set to 0, because dose values within the cavity are due to an imaging artifact. Additionally, reconstruction artifacts resulted in dose values less than 0; therefore, for analysis purposes, in post-imaging MATLAB analysis, these negative values were set to 0 so as not to alter the actual dose readings. As shown in Figure 18, the overall trend of dose fall-off for the normalized profiles reflects that of the simulation.

4. Discussion and Conclusions

4.1 Discussion

4.1.1 Experimental Results

As seen in the asymmetry in Figures 15A and 17A, the cavity was not inserted perfectly perpendicular to surface of PRESAGE during the molding process, causing the cavity to be a slight angle. This results in asymmetry in the sagittal and coronal views, as well as the axial dose deposition being off center. Translations were applied to the simulation image during the 1D and 2D analysis to correct for this. The dose distribution of the experiment has a higher gradient, but has same general $1/r^2$ dependence as the simulation, as seen in the normalized plots in Figures 16 and 18. The initial aim was to achieve 1Gy of dose 1cm away from the source. This goal was not met, so a different axial slice was analyzed to compare the relative dose distribution. The signal may not be as strong as expected due to the fading of the signal over time. While PRESAGE has been shown to be relatively stable for up to 90 hours post-irradiation, this phantom was sitting for slightly longer, resulting in probable fading and as a result, a lower dose value. This may explain the overall lower dose distribution and the absence of dose 1cm away.

Previous studies have shown the use of the DMicros system to have an absolute dose agreement for PRESAGE within 5% of the calculated plan. Discrepancies may be attributed to several factors, including the measurement devices and the characteristics

of the cuvettes versus the dosimeter volumes. The spectrophotometer may have a slightly different illumination spectrum than the optical CT system due to the use of a prism to split the white light source into the different wavelengths and selecting out the desired 633nm. The other possible cause of discrepancy is the ageing and sensitivity characteristics of the very small cuvette volumes in comparison with the much larger dosimeter volumes. The different rate of curing of the polymer is believed to result in small differences in the polymer lattice strength.[21] Due to these factors and the signal fading, the preliminary results from this study is instead used to analyze the relative dose distribution using the normalized curves as opposed to using it as a standard for comparing absolute dose.

Figure 15B and 17B show how the imaging artifacts create spikes in the data that may be interpreted as dose. In normal CT, ring artifacts are attributed to a dead pixel. In optical CT however, these artifacts are more likely due to refraction of light due to the complex geometry of the object. Figure 17A and B show dose still within the cavity even after removal of the solution. Using the original CT scan, a mask can be generated and registered with the reconstructed image in order to set the values within the cavity to 0. This would allow for a more accurate dose profile and peak value, as the bright imaging artifacts are counted as dose. Once these are eliminated, the normalization where the pixel values are divided by the maximum will be a better reflection of the dose profile. Noise may have been amplified due to the conversion into frequency space for the fast

Fourier transform and convolution algorithm. Filtering the image before the transform to reduce the noise will minimize the amplification effect that makes the noise more significant and misleading.

4.1.2 Simulation Results

The simulation assumed the ELP solidified in the bottom half of the injection volume, and so was designed to be six pixels high with a five-pixel radius in the 60x60x80 3D matrix with 0.1cm resolution. The results agreed with the relative dose distribution and a $1/r^2$ dose decrease, as shown in Figure 15D and 17D. The kernel is optimized for the PRESAGE material due to its assumption of a uniform medium.

4.2 Current Limitations and Future Work

This work demonstrated the feasibility of using PRESAGE as a means to measure the dose deposition from radionuclide-tagged ELP. However, several more experiments must be done before using it as reference for dosimetry purposes. We modeled the most basic geometry in a homogenous phantom, which is a solid starting point, but future studies should have increasing complexity to get a better analysis on how the ELP behave in actual tissue. This includes using multiple injection points, non-uniform or asymmetrical cavities, and unique geometries to better simulate a real injection. This would subsequently require alterations to the simulation to better match the experimental parameters.

Additional work to validate the model includes using a μSPECT scanner to obtain the activity of the injection in the phantom. The resultant activity map would be the direct input into the algorithm to allow for a more accurate simulation. There has been some uncertainty in the tissue equivalency of PRESAGE especially at very low energies, so further validation using film can be done. Another area of improvement includes minimizing the ring artifacts on the reconstructed image to allow for smoother and more accurate dose profiles.

The radionuclide I-131 is more widely implemented therapeutically due to its mode of beta decay.[16] Therefore, future studies using PRESAGE to analyze the dose distribution of I-131 tagged-ELP can be performed. However, there may be difficulties visualizing the dose distribution in PRESAGE due to its emission properties- 90% is emitted as beta radiation that causes tissue damage but does not contribute to visual dose, the remaining 10% is gamma radiation with a penetration depth on the scale of millimeters.[16] I-125 is used in laboratory settings due to its longer half-life and no beta emission, so it would still be the primary tagging element whereas the I-131 would be a concurrent study.

4.3 Conclusion

We have developed the first experimental method to verify the dose distribution of radionuclide tagged ELP using PRESAGE. This study developed a novel workflow to analyze the dose deposition and gain a better understanding of the behavior of the ELP.

Future studies can use this foundation as the basis of further analysis of more complex geometries, and to examine the effects of using various therapeutic and imaging radionuclides. Gel polymers have tended to be avoided in the past due to oxygen dependency and limited sensitivity at low doses. However, with a tissue equivalent formulation of PRESAGE, 3D dosimetry of LDR sources via this radiochromic dosimeter is now a more feasible option.

References

1. McDaniel JR, Callahan DJ, Chilkoti A. Drug delivery to solid tumors by elastin-like polypeptides. *Advanced drug delivery reviews*. 2010;62(15):1456-1467. doi:10.1016/j.addr.2010.05.004.
2. Liu W, McDaniel JR, Li X, et al. Brachytherapy using injectable seeds that are self assembled from genetically encoded polypeptides in situ. *Cancer research*. 2012;72(22):5956-5965. doi:10.1158/0008-5472.CAN-12-2127.
3. Gorjiara, T., Hill, R., Kuncic, Z., Adamovics, J., Bosi, S., Kim, J.-H. and Baldock, C. (2011), Investigation of radiological properties and water equivalency of PRESAGE® dosimeters. Med. Phys., 38: 2265–2274. doi:10.1118/1.3561509.
4. Mostaar, A., Hashemi, B., Zahmatkesh, M., Aghamiri, S., Mahdavi., S. (2010) A basic dosimetric study of PRESAGE: the effect of different amounts of fabricating components on the sensitivity and stability of the dosimeter. Phys. Med. Biol., 55: 903-912. doi:10.1088/0031-9155/55/3/023.
5. Guo, P. Y., Adamovics, J. A. and Oldham, M. (2006), Characterization of a new radiochromic three-dimensional dosimeter. Med. Phys., 33: 1338–1345. doi:10.1118/1.2192888.
6. Adamson, J., Yang, Y., Juang, T., Chisholm, K., Rankine, L., Adamovics, J., Yin, F.F., and Oldham, M. (2014), On the feasibility of polyurethane based 3D dosimeters with optical CT for dosimetric verification of low energy photon brachytherapy seeds. Med.Phys., 41: n/a, 071705. doi:10.1118/1.4883779.
7. Adamson, J., Newton, J., Yang, Y., Steffey, B., Cai, J., Adamovics, J., Oldham, M., Chino, J., and Craciunescu, O. (2012), Commissioning a CT-compatible LDR tandem and ovoid applicator using Monte Carlo calculation and 3D dosimetry. Med. Phys., 39: 4515-4523. doi:10.1118/1.4730501.
8. Vidovic, A., Juang, T., Meltsner, S., Adamovics, J., Chino, B., Steffey, B., Craciunescu, O., and Oldham, M. (2014) An investigation of a PRESAGE in vivo dosimeter for brachytherapy. Phys. Med. Biol., 59: 3893-3905. doi:10.1088/0031-9155/59/14/3893.
9. MacEwan, S. R. and Chilkoti, A. (2010), Elastin-like polypeptides: Biomedical applications of tunable biopolymers. Biopolymers, 94: 60–77. doi:10.1002/bip.21327.
10. Valiaev A, Lim DW, Schmidler S, Clark RL, Chilkoti A, Zauscher S. Hydration and Conformational Mechanics of Single, End-Tethered Elastin-like Polypeptides. *Journal of the American Chemical Society*. 2008;130(33):10939-10946. doi:10.1021/ja800502h.

11. Kowalczyk T, Hnatuszko-Konka K, Gerszberg A, Kononowicz AK. Elastin-like polypeptides as a promising family of genetically-engineered protein based polymers. *World Journal of Microbiology & Biotechnology*. 2014;30(8):2141-2152. doi:10.1007/s11274-014-1649-5.

12. Fuller, D., Koziol, J., Feng, A. (2004), Prostate brachytherapy seed migration and dosimetry: analysis of stranded sources and other potential predictive factors. Brachytherapy, 3: 10-19. doi:10.1016/j.brachy.2004.02.003.

13. Sakhalkar, H. S., Adamovics, J., Ibbott, G. and Oldham, M. (2009), A comprehensive evaluation of the PRESAGE/optical-CT 3D dosimetry system. Med. Phys., 36: 71–82. doi:10.1118/1.3005609.

14. Jackson, J., Juang, T., Adamovics, J., and Oldham, M. (2015), An investigation of PRESAGE 3D dosimetry for IMRT and VMAT radiation therapy treatment verification. Phys. Med. Biol., 60: 2217-2230. doi:10.1088/0031-9155/60/6/2217.

15. Rivard, M., Coursey, B., DeWerd, L., Hanson, W., Huq, M., Ibbott, G., Mitch, M., Nath, R., Williamson, J. (2004), Update of AAPM Task Group No. 43 Report: A revised AAPM protocol for brachytherapy dose calculations. Med. Phys., 31: 633-674. doi:0094-2405.

16. Robbins, J. & Schneider, A.B. Rev Endocr Metab Disord (2000) 1: 197. doi:10.1023/A:1010031115233

17. Trabbic-Carlson, K., Meyer, D., Liu, L., Piervincenzi, R., Nath, N., LaBean, T., Chilkoti, A. (2004), PEDS, 17: 57-66. doi:10.1093

18. Giap H, et al. "Validation of a dose-point kernel convolution technique for internal dosimetry." Phys. Med. Biol. 40, no. 3 (1995): 365-381

19. Furhang, E., Sgouros, G., Chen, C. (1996) "Radionuclide photon dose kernels for internal emitter dosimetry." Med Phys., 23: 759-763.

20. Lafata, Kyle. (2015) “Development of an Image-Guided Dosimetric Planning System for Injectable Brachytherapy using ELP Nanoparticles.” DukeSpace, http://hdl.handle.net/10161/10034.

21. Thomas, A., Newton, J., Adamovics, J. and Oldham, M. (2011), Commissioning and benchmarking a 3D dosimetry system for clinical use. Med. Phys., 38: 4846–4857. doi:10.1118/1.3611042